

Neutral quark matter in a Nambu–Jona-Lasinio model with vector interactionH. Abuki,^{1,*} R. Gatto,^{2,†} and M. Ruggieri^{3,‡}¹*Institut für Theoretische Physik, J. W. Goethe Universität, D-60438 Frankfurt am Main, Germany*²*Département de Physique Théorique, Université de Genève, CH-1211 Genève 4, Switzerland*³*INFN, Sezione di Bari, I-70126 Bari, Italy*

(Received 14 April 2009; published 19 October 2009)

We investigate the three flavor Nambu–Jona-Lasinio model of neutral quark matter at zero temperature and finite density, taking into account the scalar, the pseudoscalar, and the Kobayashi-Maskawa-’t Hooft interactions as well as the repulsive vector plus axial-vector interaction terms (vector extended Nambu—Jona-Lasinio). We focus on the effect of the vector interaction on the chiral restoration at finite density in neutral matter. We also study the evolution of the charged pseudoscalar meson energies as a function of the quark chemical potential.

DOI: [10.1103/PhysRevD.80.074019](https://doi.org/10.1103/PhysRevD.80.074019)

PACS numbers: 12.38.Aw, 12.38.Mh

I. INTRODUCTION

Quantum chromodynamics (QCD) is accepted nowadays as the theory of strong interactions. The phase diagram of strongly interacting matter in the $T - \mu$ plane, where T, μ denote, respectively, the temperature and the baryon chemical potential, is one of the most intriguing research topics in modern theoretical physics. Investigations on the various phases of the QCD phase diagram enlighten the physics of high temperature and small density, as well as small temperature and large density, matter: the former can be created in our laboratories by means of heavy ions collisions; the latter may be realized in the cores of the compact stellar objects (white dwarfs and neutron stars). The equation of state of strongly interacting matter is all that one needs to make theoretical predictions in the whole $T - \mu$ regime. Unfortunately, QCD is analytically treatable only in the perturbative regime. Moreover, the most interesting phenomena are not of a perturbative nature. For this reason, the QCD equation of state is only known in a small slice of the phase diagram.

The most concrete knowledge about strong interactions at $\mu = 0$ comes from lattice QCD (LQCD). However, at $\mu > 0$ LQCD calculations with three colors suffer from the sign problem. In order to circumvent this problem several approaches have been suggested: expansion in μ/T [1,2], reweighting techniques [3], and analytical continuation from the imaginary chemical potential axes [4,5]. However, none of them has yet been of a practical use at high chemical potential and small temperature region. Therefore, to make theoretical investigations on the QCD phase diagram, and to compute the equation of state in a wider range of chemical potentials where perturbative QCD does not work, some effective models are needed.

Among them the Nambu—Jona-Lasinio (NJL) model [6–9] is probably the most popular one: it shares the global symmetries of QCD and is simpler to handle than QCD itself. The main characteristic of the QCD vacuum, that is spontaneous breaking of the chiral symmetry, is described in the NJL model in a clear way. Moreover, its minimal extension to the Polyakov-NJL model [10,11] reproduces LQCD results at $\mu = 0$ as well as at small chemical potential [12] and at imaginary chemical potential [13]. As a consequence the NJL model is a promising tool to make calculations of the QCD phase diagram.

In this work, we investigate the three flavor Nambu–Jona-Lasinio model of neutral and β -equilibrated quark matter at zero temperature and finite density, taking into account the scalar, the pseudoscalar, and the Kobayashi-Maskawa-’t Hooft interactions [14,15] as well as the repulsive vector plus axial-vector interaction terms [16–19]. The introduction of the vector interaction and thus of the vector excitations is interesting for several reasons: first, it is well known that vector interactions play a dominant role in determining the properties of matter at intermediate densities. Experimental progress on the measurements of the in-medium properties of vector mesons can be found in Refs. [20,21]. In these conditions of baryon densities the main degrees of freedom are nucleons and the lighter pseudoscalar mesons (π and K), interacting among them by the exchange of vector mesons (mainly ρ and ω). One may wish to derive meson-baryon interactions starting from a microscopic interacting theory of the constituent quarks. Such a derivation can be obtained by means of the well-known bosonization and hadronization of the NJL Lagrangian [22,23]. Keeping in mind the relevance of vector meson modes on the phenomenology of nuclear matter at intermediate densities, the vector interaction (which excites vector and pseudovector mesons) must be included from the very beginning in the hadronization of the NJL Lagrangian. Second vector meson exchange might be responsible for kaon condensation at high density. With respect to this phenomenon, it is of a certain interest to

*abuki@th.physik.uni-frankfurt.de

†raoul.gatto@physics.unige.ch

‡marco.ruggieri@ba.infn.it

compare the scenario offered by the NJL model with that obtained within the hidden local symmetry framework, the latter being consistent with kaon condensation [24–27]. Third, it has been suggested that quark hadron continuity can be realized by means of the spectral function continuity of the vector mesons [28].

These are only some of the reasons that lead us to consider the role of the vector interaction in quark matter, with particular focus on neutral and β -equilibrated systems which should be realized in the core of neutron stars, if it exists.

We study in this work the extended NJL model with vector interaction, with particular emphasis put on the neutral and equilibrated quark matter. The role of the vector interaction in the NJL model has been studied several times [16–19,29–31], but not yet in the regime of electrical neutrality and β equilibrium. The study of neutral, as well as β -equilibrated, matter is interesting for astrophysical applications: matter inside a compact star has to be electrically neutral; moreover, since weak processes have a small characteristic time compared to the lifetime of a compact star, matter inside it should be equilibrated with respect to weak interactions also. We can anticipate one of the results of our study; namely, the phase diagram we compute does not differ qualitatively from that found in the aforementioned references. However, this does not diminish the relevance of our work. As a matter of fact, if one wishes to study the ground state of the model, having in mind physical applications such as, for example, the structure of the compact stellar objects, then neutrality is a necessary requirement that must be settled on, and not a mere academic problem.

The vector coupling G_V in the vacuum can be determined by the fit of the vector meson spectrum. However, it is not clear if G_V in the nuclear medium has the same value it has in the vacuum [31]. Experimental data on the medium modifications of the ω vector meson mass [21] for densities up to the saturation nuclear density can be reproduced within a NJL model with a fixed value of G_V but with additive multi-quark interactions [32,33]; the effect of these interactions can be rephrased simply as density dependent redefinitions of the coupling constants [32–35]. As a consequence it is not wrong to think of a model in which only four quark interactions are included but where the coupling constants run with density. Instead of computing G_V at each value of the chemical potential, in this work we treat it as a free parameter, and investigate its influence on the restoration of the approximate chiral symmetry at finite density. NJL studies with $G_V = 0$ predict a first order chiral restoration at μ of the order of the constituent quark masses. When G_V is switched on, if its magnitude is larger than a critical value, then the transition becomes a smooth crossover [19]. We reproduce this scenario with neutral matter at equilibrium. Also, a strong enough vector interaction disfavors the existence of the critical end point of the phase diagram [31].

We do not include color superconductivity in this study. This is done for simplicity. Nevertheless our results for the electron chemical potential and for the densities of the various species bear some implication of the effects of the repulsive vector interaction in the color superconductive phases. A quantitative study on the role of vector (as well as multi-quark) interaction on the two flavor color superconductor has been performed in Refs. [30,35], but an analogous study in realistic three flavor quark matter is still missing.

Another point that we consider in some detail is the spectrum of the pseudoscalar excitations. This subject has been considered, within the NJL model but in the non-neutral case, in Ref. [36]. We first derive the loop expansion of the meson action. It includes scalar, pseudo-scalar, vector, and pseudovector mesons. However, we focus here only on the pseudoscalar modes; therefore, we specialize our equations to this case. We leave a more complete study to a future work. This choice is motivated by the comparison we would be tempted to make with nuclear matter models, which predict a kaon condensed phase for densities in the range $(2.5-5)\rho_0$ [37]. We anticipate another result, namely the absence of strangeness condensation even in the presence of a vector interaction, although the vector interaction lowers the K^- in-medium energy. This result was anticipated in Ref. [36]. However, the authors of this paper do not make any attempt to compute the chemical potential felt by the kaons, which is a relevant ingredient to exclude definitely meson condensation in the ground state, since they are not interested to the neutral phases. Moreover, they made their analysis on the basis of the low density approximation within the lowest linear level in ρ/ρ_0 . Even though at this order some model independent prediction is possible, one might be rather interested in the outcome of the model without any further approximations other than the random phase approximation together with the mean field approximation.

With this in mind, our work improves, and at the same time confirms, the results of Ref. [36], since we compute on the same footing both the meson masses and their effective chemical potentials, in the neutral phases. Moreover, at large enough density we find a new collective mode with K^- quantum number but with lower mass, standing just below the Landau damping threshold. This is an unexpected feature of the model, which comes out after the low density approximation is relaxed. Even if we cannot exclude the possibility that this new excitation is just a model artifact, it should be stressed that it might modify the arguments about the critical baryon density for the onset of strangeness, and therefore it might even bring a drastic change in the conventional picture for the population of strangeness in the compact stars.

We also compare the NJL scenario studied here with that of a simple nuclear model in which kaon condensation is realized [38,39]; this comparison is useful since it suggests

the possible directions to follow in order to reproduce, at least qualitatively, the scenario accepted by the nuclear matter physics community. For completeness we notice that other studies exist in which the kaon condensation scenario is not favored [40].

The plan of the paper is as follows: in Sec. II we specify the Lagrangian of the vector extended NJL (VENJL) model. In Sec. III we derive the mean field effective action of the VENJL model as well as the effective action for the meson excitations at the second order in the meson fields. In Sec. IV we show results for the restoration of the approximate chiral symmetry at finite baryon chemical potential. In Sec. V we present a detailed discussion of the charged pseudoscalar modes in neutral and β -equilibrated quark matter. In Sec. VI, inspired by our results, we briefly discuss on the role that vector interaction might have on color superconductivity. Finally, in Sec. VII we summarize our results and draw our conclusions.

II. VENJL MODEL

In this work we are interested in neutral and β -equilibrated quark matter at finite density. We work in the grand canonical ensemble formalism, introducing a chemical potential μ corresponding to the conserved baryon number. To be more specific we consider a system of u , d , and s quarks at a finite chemical potential μ described by the Lagrangian

$$\begin{aligned} \mathcal{L} = & \sum_f \bar{\psi}_f [i\partial_\mu \gamma^\mu + \mu \gamma_0] \psi_f + \mathcal{L}_{\text{mass}} + \mathcal{L}_4 + \mathcal{L}_6 \\ & + \mathcal{L}_V + \mathcal{L}_A + \bar{e} [i\partial_\mu \gamma^\mu] e, \end{aligned} \quad (1)$$

where ψ_f corresponds to the quark field with flavor f ($= 1, 2, 3$ for u, d, s) and e denotes the electron field. We now specify each term in Eq. (1). A sum over color indices is understood in Eq. (1).

Equilibrium under weak interactions $d \rightarrow ue\bar{\nu}$, $s \rightarrow ue\bar{\nu}$ implies $\mu_d = \mu_s$ and $\mu_d = \mu_u + \mu_e$ (we assume neutrinos escape from matter; therefore, $\mu_\nu = 0$ ¹). Moreover, in order to achieve electrical neutrality we introduce the Lagrange multiplier μ_Q associated with the total charge Q , add the term $\mu_Q \hat{Q}$ to the Lagrangian (1), and minimize the thermodynamic potential under the stationarity condition $\partial\Omega/\partial\mu_Q = 0$. The total charge operator is given by

$$\hat{Q} = \frac{2}{3} u^\dagger u - \frac{1}{3} d^\dagger d - \frac{1}{3} s^\dagger s - e^\dagger e, \quad (2)$$

thus adding $\mu_Q \hat{Q}$ to Eq. (1) and recognizing that $\mu_Q = -\mu_e$ we get the chemical potentials of the quarks, namely,

¹Some interesting possibilities may also arise when the neutrinos are trapped in the very early stage of the thermal evolution of protoneutron stars before the deleptonization. The readers are referred to [41–44] in this context.

$$\mu_u = \mu - \frac{2}{3}\mu_e, \quad \mu_d = \mu_s = \mu + \frac{1}{3}\mu_e. \quad (3)$$

Next we describe the other terms in our Lagrangian (1). The mass term is

$$\mathcal{L}_{\text{mass}} = -\sum_f m_f \bar{\psi}_f \psi_f \quad (4)$$

and m_f is the current mass. In this work we assume $m_u = m_d$. The NJL four-fermion and six-fermion interaction Lagrangians are [7–9]

$$\mathcal{L}_4 = G \sum_{a=0}^8 [(\bar{\psi} \lambda_a \psi)^2 + (i\bar{\psi} \gamma_5 \lambda_a \psi)^2], \quad (5)$$

$$\mathcal{L}_6 = -K [\det \bar{\psi}_f (1 + \gamma_5) \psi_{f'} + \det \bar{\psi}_f (1 - \gamma_5) \psi_{f'}], \quad (6)$$

where λ_a are the Gell-Mann matrices in flavor space ($\lambda_0 = \sqrt{2/3}1_f$) and the determinant is in flavor space as well.

Finally, $\mathcal{L}_V + \mathcal{L}_A$ denote the following $U(3)_V \otimes U(3)_A$ invariant interaction term:

$$\mathcal{L}_V + \mathcal{L}_A = -G_V \sum_{a=0}^8 [(\bar{\psi} \gamma^\mu \lambda_a \psi)^2 + (\bar{\psi} \gamma^\mu \gamma_5 \lambda_a \psi)^2], \quad (7)$$

where a summation over color and flavor is understood. In the above equation λ_a denote the same set of matrices in the flavor space introduced in Eq. (1). Typical values of G_V in the vacuum are $0.2 \leq G_V/G \leq 3$ [16,19,29,32,35].

III. EFFECTIVE POTENTIAL AND EFFECTIVE ACTION OF MESONS

In this section we sketch the derivation of the mean field effective potential as well as of the effective action of the meson modes in the VENJL model. The derivation is done in some detail in order to easily compare our notations and results with the existing literature. We follow the conventions of Ref. [7].

The easiest way to derive the meson propagators is the so-called linear approach [45–47]. First, we write the t' Hooft term as an effective 4-fermion interaction: this is a well-known procedure [7]; therefore, we do not insist on its details. After this is achieved the scalar and pseudoscalar interaction is written as

$$\begin{aligned} \mathcal{L}_4 + \mathcal{L}_6 = & \sum_{a=0}^8 [K_a^{(-)} (\bar{\psi} \lambda_a \psi)^2 + K_a^{(+)} (\bar{\psi} i\gamma_5 \lambda_a \psi)^2] \\ & + \mathcal{L}_{\text{mixing}}, \end{aligned} \quad (8)$$

where the term $\mathcal{L}_{\text{mixing}}$ generates the mixing between π^0 , η^0 , and η^8 modes and is not important in this context since we focus on the charged meson modes. The effective coupling constants are defined as follows:

$$K_0^{(\pm)} = G \mp \frac{K}{3}(-\sigma_s - \sigma_u - \sigma_d), \quad (9)$$

$$K_1^{(\pm)} = K_2^{(\pm)} = K_3^{(\pm)} = G \pm \frac{K}{2}(-\sigma_s), \quad (10)$$

$$K_4^{(\pm)} = K_5^{(\pm)} = G \pm \frac{K}{2}(-\sigma_d), \quad (11)$$

$$K_6^{(\pm)} = K_7^{(\pm)} = G \pm \frac{K}{2}(-\sigma_u), \quad (12)$$

$$K_8^{(\pm)} = G \mp \frac{K}{6}(-\sigma_s + 2\sigma_u + 2\sigma_d). \quad (13)$$

In the above equations $\sigma_f = \langle \bar{f}f \rangle$. Then we define the following meson fields:

$$\phi_a = K_a^{(-)} \bar{\psi} \lambda_a \psi, \quad (14)$$

$$\pi_a = K_a^{(+)} \bar{\psi} i \gamma_5 \lambda_a \psi, \quad (15)$$

$$v_a^\mu = G_V \bar{\psi} \gamma^\mu \lambda_a \psi, \quad (16)$$

$$a_a^\mu = G_V \bar{\psi} \gamma^\mu \gamma_5 \lambda_a \psi. \quad (17)$$

The partition function of the model can be cast in the form [47]

$$Z = \int \mathcal{D}M \mathcal{D}\psi \mathcal{D}\bar{\psi} e^{iS}, \quad \mathcal{D}M \equiv \mathcal{D}\phi \mathcal{D}\pi \mathcal{D}v \mathcal{D}a, \quad (18)$$

with the bosonized action given by

$$\begin{aligned} S = & \int d^4x \bar{\psi} [i \gamma^\mu \partial - m + 2\phi_a \bar{\psi} \lambda_a \psi + 2\pi_a \bar{\psi} i \gamma_5 \lambda_a \psi \\ & - 2v_a^\mu \bar{\psi} \gamma_\mu \lambda_a \psi - 2a_a^\mu \bar{\psi} \gamma_\mu \gamma_5 \lambda_a \psi] \psi \\ & - \int d^4x \left[\frac{\phi_a^2}{K_a^{(-)}} + \frac{\pi_a^2}{K_a^{(+)}} \right] + \int d^4x \left[\frac{v_a^2 + a_a^2}{G_V} \right]. \quad (19) \end{aligned}$$

In Eq. (19) we have not shown explicitly the contribution of the free electron gas (it will be inserted at the end of the calculation). At this stage the meson fields are external fields (i.e., with no kinetic term). Their kinetic terms as well as their interactions will arise once the fermions are integrated out. Before performing this integral we notice that in our application we expect condensation in some of the ϕ_a and v_a^μ channels. These condensations are related to chiral condensates of the three flavors and to fermion densities. Thus we define

$$\phi_a = \sigma_a + \delta_a, \quad (20)$$

$$v_a^\mu = V_a^\mu + \rho_a^\mu, \quad (21)$$

with $a = 0, \dots, 8$ and $\langle \delta_a \rangle = \langle \rho_a^\mu \rangle = 0$. With this choice $\mathcal{D}M = \mathcal{D}\delta \mathcal{D}\pi \mathcal{D}\rho \mathcal{D}a$, and the physical meson fields

will be identified with the fluctuations around their expectation value. In principle we should introduce expectation values for charged pseudoscalar mesons as well, since their in-medium energies can be lower than the threshold of condensation. However, we first study the system without the assumption of charged pseudoscalar meson condensation: as long as we exclude the possibility of first order transition [48,49], the evolution of their rest energies as a function of the baryon density will allow us to establish whether condensation occurs or not (see the next section for more details).

The functional integration over $\mathcal{D}\psi \mathcal{D}\bar{\psi}$ in the partition function can be done exactly since the action (19) is quadratic in the fermion fields. Using textbook relations we get

$$Z = \int \mathcal{D}M e^{iS[\phi, \pi, v, a]}, \quad (22)$$

with the effective action $S[\phi, \pi, v, a]$ given by

$$\begin{aligned} S[\phi, \pi, v, a] = & -i \text{Tr} \log [S_0^{-1} + 2\delta_a \lambda_a + 2i\pi_a \gamma_5 \lambda_a \\ & - 2\rho_a^\mu \gamma_\mu \lambda_a - 2a_a^\mu \gamma_\mu \gamma_5 \lambda_a] \\ & - \int d^4x \left[\frac{\sigma_a^2 + \delta_a^2 + 2\delta_a \sigma_a + \frac{\pi_a^2}{K_a^{(+)}}}{K_a^{(-)}} \right] \\ & + \int d^4x \left[\frac{V_a^2 + \rho_a^2 + 2V_a \rho_a + a_a^2}{G_V} \right], \quad (23) \end{aligned}$$

and

$$S_0^{-1} = i \gamma_\mu \partial^\mu - m + \mu \gamma_0 + 2\sigma_a \lambda_a - 2V_a^\mu \gamma_\mu \lambda_a. \quad (24)$$

For the sake of compactness we introduce the total fluctuating meson field

$$\mathcal{M}_a = \delta_a + i\pi_a \gamma_5 - \rho_a^\mu \gamma_\mu - a_a^\mu \gamma_\mu \gamma_5. \quad (25)$$

Expanding the log term we finally cast the effective action in the form

$$\begin{aligned} S[\phi, \pi, v, a] = & S_{\text{MF}} - i \sum_{n=1}^{\infty} \frac{(-1)^{n+1}}{n} \text{Tr} [(S_0 2\lambda_a \mathcal{M}_a)^n] \\ & - \int d^4x \left[\frac{\delta_a^2 + 2\delta_a \sigma_a + \frac{\pi_a^2}{K_a^{(+)}}}{K_a^{(-)}} \right] \\ & + \int d^4x \left[\frac{\rho_a^2 + 2V_a \rho_a + a_a^2}{G_V} \right], \quad (26) \end{aligned}$$

where S_{MF} denotes the contribution of the effective action that does not depend on the fluctuating fields,

$$S_{\text{MF}} = -i \text{Tr} \log S_0^{-1} - \int d^4x \left[\frac{\sigma_a^2}{K_a^{(-)}} \right] + \int d^4x \left[\frac{V_a^2}{G_V} \right]. \quad (27)$$

The sum in Eq. (26) is a loop expansion that generates the

kinetic terms for the mesons as well as their interactions. We now examine S_{MF} and this loop expansion separately.

A. Mean field effective potential

We now focus on the mean field term in Eq. (27). First, we have to specify the expectation values in Eqs. (20) and (21). We assume that in the ground state condensation occurs only in the channels $\langle \bar{f}f \rangle$ and $\langle f^\dagger f \rangle$ (the latter being relevant at finite quark density). Here f denotes the quark with flavor f . This implies that in Eqs. (20) and (21) only the terms with $a = 0, 3, 8$ and $\mu = 0$ survive, the remainders being zero. It is easy to show that S_0^{-1} takes the simple form

$$S_0^{-1} = \begin{pmatrix} h_u & 0 & 0 \\ 0 & h_d & 0 \\ 0 & 0 & h_s \end{pmatrix}, \quad (28)$$

where

$$h_f = (p_0 + \mu_f - 4G_V \rho_f) \gamma_0 - \mathbf{p} \cdot \boldsymbol{\gamma} - M_f, \quad (29)$$

and

$$M_f = m_f - 4G\sigma_f + 2K\sigma_{f+1}\sigma_{f+2} \quad (30)$$

denotes the mean field (or constituent) quark mass. In the above equation

$$\sigma_f = -iN_c \text{Tr} S_f \quad (31)$$

denotes the chiral condensate of the flavor f , where S_f is the propagator of the quark of flavor f , N_c is the number of colors, and the trace is on spinor indices only. Also, we have defined $\sigma_4 = \sigma_u$, $\sigma_5 = \sigma_d$. Analogously $\rho_f = \langle f^\dagger f \rangle$ denotes the number density of f .

From Eq. (29) the role of the vector interaction in the mean field approximation is clear: it shifts the quark chemical potentials (3) to

$$\mu_f \rightarrow \mu_f - 4G_V \rho_f. \quad (32)$$

Thus, depending on the sign of G_V , the chemical potentials will be shifted either upwards or downwards once the number density $\rho_f \neq 0$.

We notice that the flavor channels λ_0 , λ_3 , and λ_8 in the vector interaction generate coupling of the quark currents to the total quark number density $\rho_u + \rho_d + \rho_s$, the isospin density $\rho_u - \rho_d$, and to the hypercharge density $\rho_u + \rho_d - 2\rho_s$, respectively. This is similar to what happens in the relativistic mean field nuclear models [38], where the coupling of the isospin nuclear current to the isovector $\boldsymbol{\rho}^\mu = (\rho_1^\mu, \rho_2^\mu, \rho_3^\mu)$ and of the nuclear current to the vector ω^μ meson gives rise at the mean field level to expectation values of the zeroth component of the ω^μ and ρ_3^μ fields, which result proportional, respectively, to the total baryon and to the isospin densities. We simply mention here that one cannot identify the vectors of the channels λ_0 , λ_3 , and λ_8 with the physical ω , ρ_0 , and ϕ fields since a mixing

among them occurs in the vacuum as well as at finite density. Keeping this in mind, with an abuse of notation, we define

$$\langle \omega^0 \rangle = G_V \langle u^\dagger u + d^\dagger d + s^\dagger s \rangle = G_V (\rho_u + \rho_d + \rho_s), \quad (33)$$

$$\langle \rho_3^0 \rangle = G_V \langle u^\dagger u - d^\dagger d \rangle = G_V (\rho_u - \rho_d), \quad (34)$$

$$\langle \phi^0 \rangle = G_V \langle u^\dagger u + d^\dagger d - 2s^\dagger s \rangle = G_V (\rho_u + \rho_d - 2\rho_s), \quad (35)$$

or equivalently

$$\rho_u = \frac{1}{6G_V} (2\langle \omega^0 \rangle + 3\langle \rho_3^0 \rangle + \langle \phi^0 \rangle), \quad (36)$$

$$\rho_d = \frac{1}{6G_V} (2\langle \omega^0 \rangle - 3\langle \rho_3^0 \rangle + \langle \phi^0 \rangle), \quad (37)$$

$$\rho_s = \frac{1}{6G_V} (2\langle \omega^0 \rangle - 2\langle \phi^0 \rangle). \quad (38)$$

The above equations allow one to rephrase the effective chemical potential in Eq. (32) in terms of the expectation values of the vector meson fields.

Finally, writing

$$e^{-\beta V \Omega} = Z \quad (39)$$

with Z given in Eq. (22), we get the mean field effective potential:

$$\Omega_{\text{MF}} = -4K\sigma_u\sigma_d\sigma_s + 2G \sum_{f=u,d,s} \sigma_f^2 - 2G_V \sum_{f=u,d,s} \rho_f^2 + V_{\log}, \quad (40)$$

with

$$V_{\log} = -T \sum_{n=-\infty}^{+\infty} \int \frac{d^3 p}{(2\pi)^3} \text{Tr} \log \left[\frac{1}{T} \begin{pmatrix} h_u & 0 & 0 \\ 0 & h_d & 0 \\ 0 & 0 & h_s \end{pmatrix} \right]. \quad (41)$$

In the above equations we have introduced a finite temperature T in order to easily handle infrared divergencies that arise when the chemical potential of the flavor f is larger than its mean field mass M_f . At the end of the calculations we make the limit $T \rightarrow 0^+$.

The ground state of the model at hand is characterized by the numerical values of the condensates and of the quark number densities. We determine the values of the chiral condensates by looking for the global minima of the total effective potential:

$$\Omega = \Omega_{\text{MF}} - \frac{\mu_e^4}{12\pi^2}, \quad (42)$$

where the second addendum on the right-hand side (rhs) is

the thermodynamic potential of the free electron gas that will neutralize the net quark charge. At a fixed value of μ we choose the value $\bar{\mu}_e$ of μ_e which neutralizes the system, which is defined by the stationarity condition

$$0 = \left. \frac{\partial \Omega}{\partial \mu_e} \right|_{\mu_e = \bar{\mu}_e}. \quad (43)$$

The complete numerical strategy will be described in the next section.

B. Effective action of meson fluctuations at the second order

We now discuss the action of meson fluctuations in Eq. (26). The term with $n = 1$, when summed to the linear terms in the second and third line of the same equation, gives rise to terms of the form $\delta_a F_a$ or $\rho_a G_a$, where F_a and G_a schematically denote the gap equations whose solutions determine the physical values of the chiral condensate and the quark number densities [47]. Since for these values both F_a and G_a vanish, the linear terms do not appear in the effective action.

Next we consider the term with $n = 2$. This gives rise to the kinetic terms of the meson fields as well as to the mixing of some of the modes. Since the linear terms vanish, we can write the effective action at the second order as

$$\begin{aligned} S[\delta, \pi, \rho, a] = & 2i \int d^4x d^4y \text{Tr}[S_0(x, y) \lambda_a \mathcal{M}_a(y) S_0(y, x) \\ & \times \lambda_b \mathcal{M}_b(x)] - \int d^4x \left[\frac{\delta_a(x)^2}{K_a^{(-)}} + \frac{\pi_a(x)^2}{K_a^{(+)}} \right] \\ & + \int d^4x \left[\frac{\rho_a(x)^2 + a_a(x)^2}{G_V} \right], \end{aligned} \quad (44)$$

where we have not written explicitly the terms proportional to σ_a^2, V_a^2 since they contribute only to S_{MF} . In the above equation the trace is understood over color, flavor, and Dirac indices.

By means of the loop expansion in Eq. (44) we could study every meson fluctuation at the second order in the meson field about the mean field solution. However, in this paper we focus our attention on the charged pseudoscalar modes, reserving a more complete study for a future paper.

The propagator of these modes is easily obtained from Eq. (44). We are interested in the rest energies of the meson modes. We have verified by a direct calculation that there is no mixing between the pseudoscalar and the longitudinal component of the pseudovector mode in the case in which we put the spatial momentum of the meson $\mathbf{Q} = 0$. Moreover, parity conservation in strong interactions is enough to ensure that mixing at the second order in the fields does not arise between pseudoscalar mesons and the vector or the scalar ones. Thus the remaining term to be computed is that of order $\mathcal{O}(\pi_a \pi_b)$ of Eq. (44). Fourier transforming both the fields and the propagators we have

$$\begin{aligned} S[\pi_a] = & - \int \frac{d^4q}{(2\pi)^4} \pi_a(-q) \pi_b(q) \\ & \times \left[\frac{\delta_{ab}}{K_b^{(+)}} + 2i \int \frac{d^4\ell}{(2\pi)^4} \right. \\ & \left. \times \text{Tr}[S_0(\ell) \gamma_5 \lambda_a S_0(\ell + q) \gamma_5 \lambda_b] \right]. \end{aligned} \quad (45)$$

Since at the second order there is no mixing among the pseudoscalar and the other fields, at least in the rest system of the mesons, we identify the matrix in parenthesis in Eq. (45) with half of the inverse meson propagator in momentum space:

$$\begin{aligned} \frac{1}{2} D_{ab}(q)^{-1} = & - \frac{\delta_{ab}}{K_b^{(+)}} - 2i \int \frac{d^4\ell}{(2\pi)^4} \\ & \times \text{Tr}[S_0(\ell) \gamma_5 \lambda_a S_0(\ell + q) \gamma_5 \lambda_b]. \end{aligned} \quad (46)$$

Consider, for example, the charged kaons whose fields are defined as

$$K^\pm = \frac{\pi_4 \pm i\pi_5}{\sqrt{2}}, \quad (47)$$

then using $D_{44}^{-1} = D_{55}^{-1} \equiv D$ and $D_{45}^{-1} = -D_{54} \equiv i\delta D^{-1}$ it is easy to show that

$$\begin{aligned} & \int \frac{d^4q}{(2\pi)^4} \frac{1}{2} (\pi_4(-q), \pi_5(-q)) \begin{pmatrix} D^{-1}(q) & i\delta D(q) \\ -i\delta D(q) & D^{-1}(q) \end{pmatrix} \\ & \times \begin{pmatrix} \pi_4(q) \\ \pi_5(q) \end{pmatrix} \\ & = \int \frac{d^4q}{(2\pi)^4} K^+(-q) (D^{-1}(q) - \delta D^{-1}(q)) K^-(q) \\ & + K^-(-q) (D^{-1}(q) + \delta D^{-1}(q)) K^+(q); \end{aligned}$$

the condition $D^{-1}(q_0 = \omega_K, \mathbf{q} = 0) - \delta D^{-1}(q_0 = \omega_K, \mathbf{q} = 0) = 0$ with ω_K being positive defines the rest energy of charged K^+ . Since $D^{-1}(-q_0, \mathbf{q}) = D^{-1}(q_0, \mathbf{q})$ and $\delta D^{-1}(-q_0, \mathbf{q}) = -\delta D^{-1}(q_0, \mathbf{q})$ can be easily shown, it follows that the negative energy solution to $D^{-1} - \delta D^{-1} = 0$ corresponds to the positive energy solution to $D^{-1} + \delta D^{-1} = 0$ indicating that we need only one equation $D^{-1} - \delta D^{-1} = 0$ to extract both the K^- and K^+ energies. Similar results hold for the remaining mesons.

IV. NEUTRAL GROUND STATE OF THE VENJL MODEL

In this section we discuss the neutral and β -equilibrated ground state of the VENJL model at zero temperature, obtained by the procedure of minimization of the effective potential Ω under the neutrality condition (43). We present results for the following set of parameters [50]:

$$m_u = m_d = 5.5 \text{ MeV}, \quad (48)$$

$$m_s = 140.7 \text{ MeV}, \quad (49)$$

$$\Lambda = 602.3 \text{ MeV}, \quad (50)$$

$$G = 1.835/\Lambda^2, \quad (51)$$

$$K = 12.36/\Lambda^5, \quad (52)$$

but the results are qualitatively similar to those that we obtain with the different set of Ref. [51]. First, we are interested in the effect of the vector interaction on the neutral ground state of the model.

The value of G_V can (and should) be fixed *in the vacuum* in order to reproduce the spectrum of the vector mesons; see, for example, [18]. However, it is not clear how large the modification of G_V is in the medium [31]; therefore, instead of fixing it by the meson spectrum in the vacuum we treat it as a free parameter in order to grasp its effects on the chiral restoration transition at finite density, as well as on the in-medium meson properties. We measure the strength of the vector interaction in terms of the scalar coupling G and introduce the ratio

$$r_V = \frac{G_V}{G}. \quad (53)$$

In the vacuum we find $r_V \approx 0.6$ in order to reproduce the neutral ρ meson mass $m_\rho = 775 \text{ MeV}$. We notice that because of the shift in Eq. (29) the quark number density for the flavor f in the mean field approximation is self-consistently defined by the equation

$$\rho_f = \frac{N_c}{3\pi^2} [(\mu - Q\mu_e - 4G_V\rho_f)^2 - M_f^2]^{3/2} \times \theta[(\mu - Q\mu_e - 4G_V\rho_f)^2 - M_f^2], \quad (54)$$

where M_f denotes the in-medium quark mass. The rhs of the above equation is nothing but the number density of a degenerate Fermi gas with a density dependent Fermi momentum given by

$$[(\mu - Q\mu_e - 4G_V\rho_f)^2 - M_f^2]^{1/2}.$$

It is interesting to note that Eq. (54) is equivalent to the partial derivative of the effective potential with respect to ρ_f , which is related to condensations of ω , ρ_0 , and ϕ through Eqs. (33)–(35); i.e.,

$$\frac{\partial \Omega_{\text{MF}}}{\partial \rho_f} = 0. \quad (55)$$

In this case Ω_{MF} should be regarded as a function of eight variables, i.e., $\{\sigma_f, \rho_f, \mu_e, \mu\}$ [30]. It turns out that the ground state is realized as the maximum with respect to variables ρ_f when $G_V > 0$ (repulsive vector interaction). However, it does not immediately mean the ground state is unstable against the vector meson fluctuation. Actually, the vector meson mode is not tachyonic, as we always find a

positive and real mass for ρ meson. This means the curvature of the effective potential cannot help us to judge if the system is unstable against small fluctuations in the vector channel. The total charge is given by

$$0 = \frac{2}{3}\rho_u - \frac{1}{3}\rho_d - \frac{1}{3}\rho_s - \rho_e, \quad (56)$$

with quark number densities identified with the solutions of Eq. (54).

Since the number densities in the case $r_V \neq 0$ have to be computed self-consistently by virtue of Eq. (54) the numerical calculations are slightly more involved than for the case $r_V = 0$. Our numerical strategy is as follows: for each value of μ we solve Eq. (54) for each flavor; this allows us to define three numerical functions $\rho_f = \rho_f(\mu_e, M_f)$, one for each flavor f . Moreover, we define a fourth numerical function which relates the physical electron chemical potential (namely the value of μ_e that corresponds to a vanishing total electric charge) to the in-medium quark masses. This is achieved by means of the total charge Eq. (56) and densities defined above. We insert the four functions into the effective potential, that now depends only on the in-medium masses (or equivalently on the chiral condensates). The global minimum of the effective potential in the space (M_u, M_d, M_s) gives the physical values of the in-medium masses. Once these are known we can step backward and compute the numerical value of μ_e and of the number densities.

The phase diagram of the model can be described equivalently in terms either of the chiral condensates or of the mean field quark masses. We prefer the latter point of view since it is physically more intuitive. From the qualitative point of view the behavior of the constituent quark masses as a function of μ is similar in the cases $r_V = 0$ and $r_V \neq 0$. In both cases there exist a critical value of μ such that M_f for $f = u, d$ suddenly decreases from its vacuum value $M_0 \approx 367 \text{ MeV}$ to a lower one, typically a few tens of MeV. However, the order of the transition depends on the value of r_V . For $r_V < 0$ we find a first order transition as in the case $r_V = 0$. In this case the critical chemical potential is lowered with respect to the case $r_V = 0$. The first order character of the transition remains even for small and positive values of r_V . At $r_V \equiv r_V^c \approx 0.5$ the first order transition becomes a crossover. In this case we identify the crossover point with the value of μ where $|dM_u/d\mu|$ is maximum. The magnitude of $|dM_u/d\mu|$ at the critical point is lowered as r_V is increased above the r_V^c , indicating that the crossover becomes more smooth. These results are in qualitative agreement with those obtained within the non-neutral and non- β -equilibrated VENJL [19,29]; they are also in agreement with the results obtained within the three flavor Polyakov-Nambu-Jona Lasinio model in Ref. [31], where it is shown that the first order line disappears from the $T - \mu$ phase diagram when G_V is increased above a critical value. We summarize these results

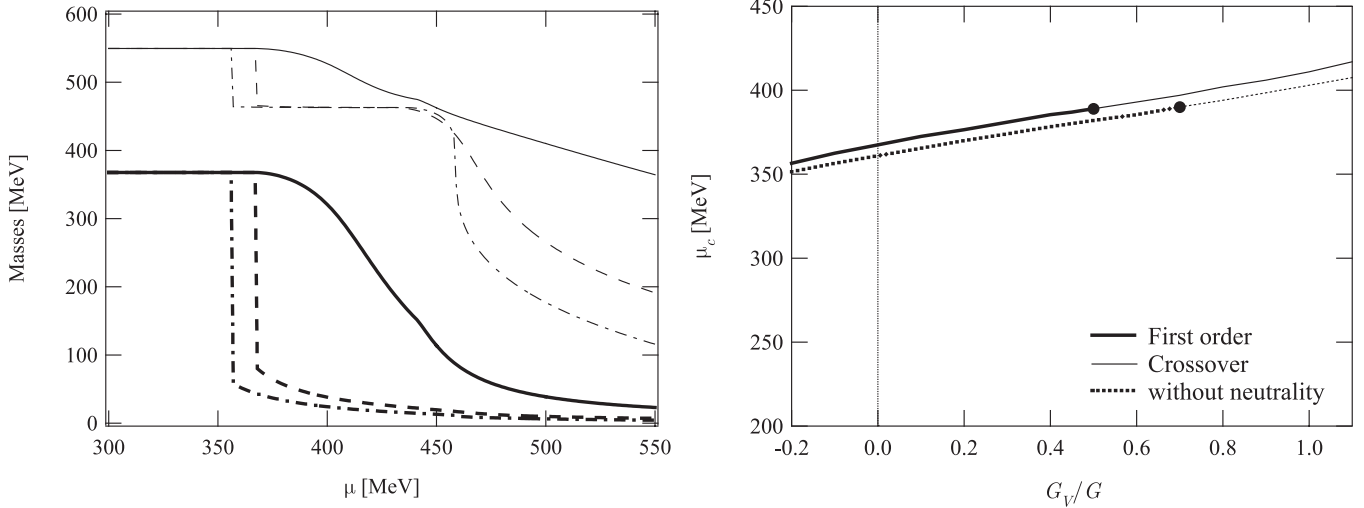


FIG. 1. Left-hand panel: Mean field up-quark mass (thick lines) and strange quark mass (thin lines) against μ for three different values of the ratio $r_V = G_V/G$ in neutral and β -equilibrated quark matter: dot-dashed line corresponds to $r_V = -0.2$, dashed line to $r_V = 0$, solid line to $r_V = +1.1$. Right-hand panel: Critical value of μ for restoration of the approximate chiral symmetry as a function of r_V . Bold line denotes first order phase transition, solid thin line corresponds to a smooth crossover. For comparison, the same quantity computed without requiring electrical neutrality is shown by dashed line.

in Fig. 1 where we plot M_u and M_s against μ for three representative values of r_V (left-hand panel), as well as the critical chemical potential as a function of r_V (right-hand panel). For comparison we plot, by dashed line in the right-hand panel of Fig. 1, the critical chemical potential computed without requiring the neutrality condition and by setting $\mu_e = 0$. We notice that the neutrality condition has an effect similar to that of the repulsive vector interaction: it stabilizes the chiral symmetry broken phase with respect to the restored phase, as it increases the critical chemical potential upwards. The same effect can also be induced by increasing the strength of repulsive vector interaction. Interestingly enough, the value of critical chemical potential at which the first order phase transition turns into a smooth crossover is not so much affected by the neutrality condition. However, the required value of the strength of repulsive vector interaction is significantly reduced if the condition of neutrality is taken into account. As a consequence, the neutrality constraint actually helps to make the transition smoother at fixed vector coupling.

In Fig. 2 we plot the baryon density ρ_B defined as

$$\rho_B = \frac{1}{3}(\rho_u + \rho_d + \rho_s) \quad (57)$$

as a function of μ for four different values of the ratio $r_V = G_V/G$. The densities of each flavor are computed by means of Eq. (54) with the values of μ_e and M_f obtained by the minimization procedure. In the figure the dot-dashed line corresponds to $r_V = -0.2$, the dashed line to $r_V = 0$, and the solid line to $r_V = 1.1$. An interesting consequence of the change from first order phase transition to crossover into the approximate chiral restored phase when $r_V \geq 0.5$ is that the baryon density as a function of μ is a continuous

function of μ . Thus the system smoothly passes from a dilute Fermi gas to a dense one, the size of the smoothness depending on the precise value of r_V . This does not happen when the transition is of first order.

In the left-hand panel of Fig. 3 we plot the electron chemical potential of neutral quark matter as a function of μ for some value of r_V . In the right-hand panel we plot the same chemical potential against the baryon density ρ_B . The latter plot is obtained by assembling data from the left-hand panel and from Fig. 2. It is interesting to notice that at a given value of μ , the larger the magnitude of r_V the larger

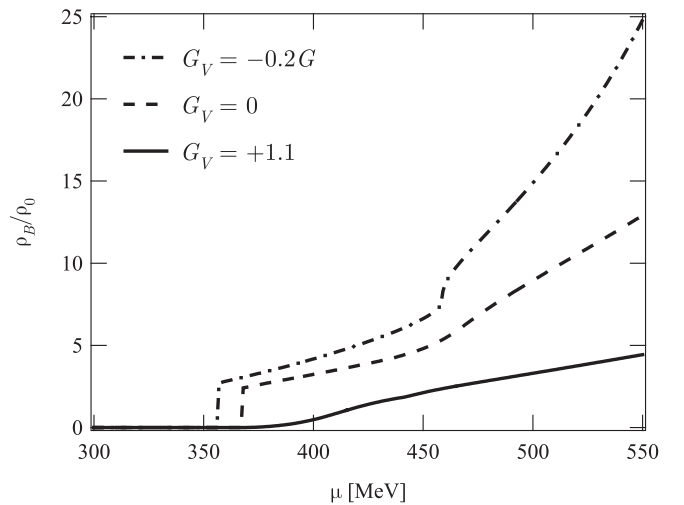


FIG. 2. Baryon density in neutral quark matter, in units of the saturation density $\rho_0 = 0.16 \text{ fm}^{-3}$, against μ for four different values of the ratio $r_V = G_V/G$: dot-dashed line corresponds to $r_V = -0.2$, dashed line to $r_V = 0$, and solid line to $r_V = 1.1$.

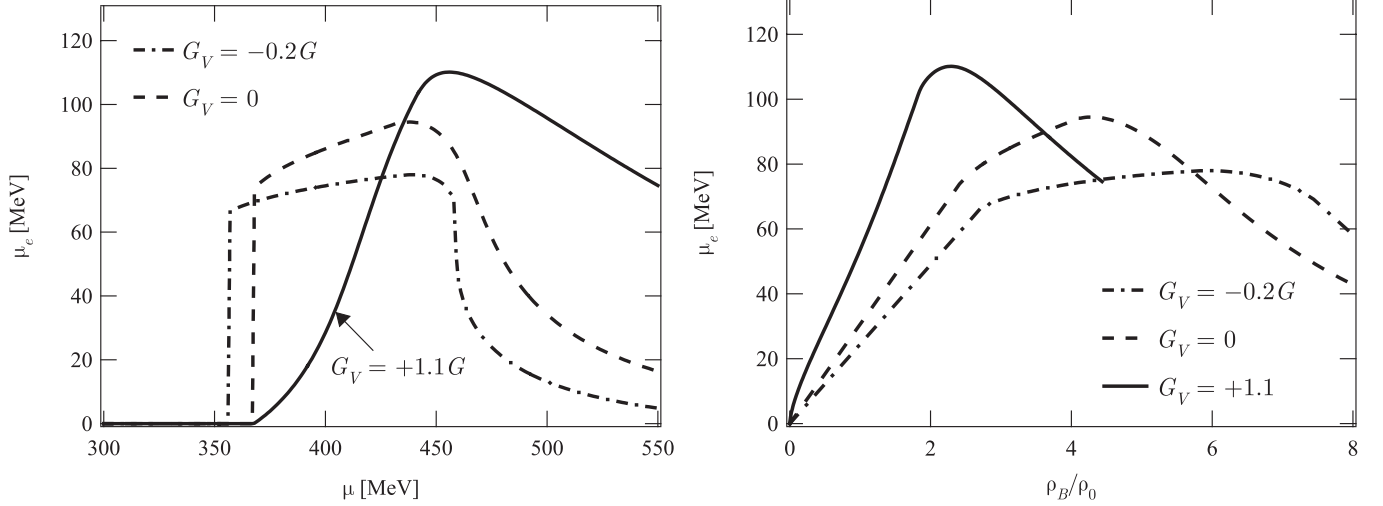


FIG. 3. Left-hand panel: Electron chemical potential in neutral quark matter against μ for four different values of the ratio $r_V = G_V/G$. Dot-dashed line corresponds to $r_V = -0.2$, dashed line to $r_V = 0$, solid line to $r_V = 1.1$. Right-hand panel: Electron chemical potential against baryon density. The line sketch is as in the left-hand panel. The change of the sign of the slope of the curves at large μ (or ρ_B) occurs in correspondence of the creation of strange quark Fermi spheres ($\mu_s > M_s$).

the numerical value of μ_e . For example, at $\mu = 440$ MeV we find $\mu_e(r_V = 0) \approx 95$ MeV, to be compared with $\mu_e(r_V = +1.1) \approx 120$ MeV. For comparison, at the same value of μ we find $\mu_e(r_V = -0.2) \approx 80$ MeV. The change of the sign of the slope of the curves at large μ (or ρ_B) occurs in correspondence with the condition $\rho_s > 0$ (at lower values of μ we find $\rho_s = 0$), which implies that strange quarks take a role in the neutralization of the system and a lower number of electrons is needed.

V. MESON ENERGIES AND (ABSENCE OF) CONDENSATION

In this section we compute the pseudoscalar meson energies as a function of the mean quark chemical potential μ at $T = 0$. To achieve this result we solve the pole equation in the rest frame for the appropriate channel as discussed in a previous section. We focus on the charged modes here because they are interesting in the context of meson condensation driven by the electron chemical potential [48,49,52–59].

Meson energies and in-medium meson propagator

Taking into account the results discussed in the previous section [see Eq. (45)] we write the equation for the energy of the charged kaons as

$$\text{Re } F_{K^\pm}(\omega) = 0, \quad F_{K^\pm}(\omega) \equiv 1 - 2K_4^{(+)} \Pi_{K^\pm}(\omega, \mathbf{0}), \quad (58)$$

where the polarization function is defined as

$$\Pi_{K^\pm}(\omega, \mathbf{Q}) = -2iN_c \int \frac{d^4 p}{(2\pi)^4} \text{Tr} \left[\gamma_5 \frac{1}{h_u(p)} \gamma_5 \frac{1}{h_s(p + \mathbf{Q})} \right], \quad (59)$$

where $Q = (\omega, \mathbf{Q})$ with \mathbf{Q} being the three momentum of kaon, and Re denotes the real part. In the above equation the trace is understood on Dirac indices only. Performing the trace the pole equation (58) in the rest frame reads:

$$24 \text{Re} \int \frac{d^3 p}{(2\pi)^3} T \sum_{n=-\infty}^{+\infty} \frac{M_u M_s + \mathbf{p}^2 - (i\omega_n + \mu_u)(i\omega_n + i\Omega_m + \mu_s)}{[(i\omega_n + \mu_u)^2 - \mathbf{p}^2 - M_u^2][(i\omega_n + i\Omega_m + \mu_s)^2 - \mathbf{p}^2 - M_s^2]} = \frac{1}{2K_4^{(+)}}. \quad (60)$$

Once again we have introduced a finite temperature T in order to handle infrared divergencies that arise when the chemical potential of the flavor f equals its mean field mass M_f . At the end of the calculation we put $T \rightarrow 0^+$. In the above equation $\Omega_m = \pi T n$ is the boson Matsubara frequency.

The retarded real time propagator is obtained via $i\Omega_m \rightarrow \omega + i0^+$ after summation over fermion Matsubara fre-

quencies. The result turns out to depend on the external energy ω only on the combination

$$Q_0 = \omega + \mu_s - \mu_u = \omega + \mu_e + 4G_V(\rho_u - \rho_s). \quad (61)$$

Thus also the kaon Lagrangian in momentum space depends only on Q_0 . This implies that in the derivative expansion one can build only terms that contain the covariant derivative

$$iD_0 \equiv i\partial_0 + \mu_e + 4G_V(\rho_u - \rho_s). \quad (62)$$

We make analytically the sum over Matsubara frequencies in Eq. (60). After continuation to real external energies we take the limit $T \rightarrow 0^+$, and we get an expression that depends on energy only through Q_0 . We do analytically the integral over $|\mathbf{p}|$. Finally we solve Eq. (60) in the variable Q_0 . The solution of the pole equation in the Q_0 variable defines the in-medium kaon mass $m_{K^\pm}^*$. Within our convention in Eq. (59) the positive (negative) energy solution of Eq. (60), $Q_0 = m_{K^-}^*$ ($Q_0 = -m_{K^+}^*$) corresponds to the K^- (K^+) in-medium mass. Once the pole equation is solved at a given value of μ , we obtain the in-medium energies trivially from Eq. (61):

$$\omega_{K^+} = \mu_e + 4G_V(\rho_u - \rho_s) + m_{K^+}^*, \quad (63)$$

$$\omega_{K^-} = -\mu_e - 4G_V(\rho_u - \rho_s) + m_{K^-}^*. \quad (64)$$

At $G_V = 0$ the chemical potential felt by kaons is $-q\mu_e$ where q denotes the electric charge (in units of the electron

charge) of the meson. When G_V is switched on, the kaon chemical potential is shifted from $-q\mu_e$ by virtue of the strong interactions. As a matter of fact, since the quark densities are related to the expectation values of the ρ , ω , and ϕ mesons, see Eqs. (36) and (38), the G_V terms in the meson energies can be interpreted as due to the interactions of kaons with the aforementioned vector mesons (there is also a modification of m_K^* when G_V is switched on). We stress, however, that these interactions do not exist at the tree level within the model we study in this work, but arise only as loop effects: the quarks interact with the expectation values of the vectors, and the quark loops, that generate the mass and the kinetic terms of the pseudoscalar mesons, will depend on these expectation values. Another source of interactions among pseudoscalar and vectors (as well as axial vectors) are the terms of the cubic order in meson fields in the loop expansion of Eq. (26), that we do not consider in this study for simplicity and will be the subject of a future paper.

The other pseudoscalar channels are treated in a similar way. The pole equation for the charged pions reads

$$24 \operatorname{Re} \int \frac{d^3 p}{(2\pi)^3} T \sum_{n=-\infty}^{+\infty} \frac{M_u M_d + \mathbf{p}^2 - (i\omega_n + \mu_u)(i\omega_n + i\Omega_m + \mu_d)}{[(i\omega_n + \mu_u)^2 - \mathbf{p}^2 - M_u^2][(i\omega_n + i\Omega_m + \mu_d)^2 - \mathbf{p}^2 - M_d^2]} = \frac{1}{2K_1^{(+)}}, \quad (65)$$

and in this case the polarization tensor depends on external energy only through the combination

$$Q_0 = \omega + \mu_d - \mu_u = \omega + \mu_e + 4G_V(\rho_u - \rho_d). \quad (66)$$

In this way we have

$$\omega_{\pi^+} = \mu_e + 4G_V(\rho_u - \rho_d) + m_{\pi^+}^*, \quad (67)$$

$$\omega_{\pi^-} = -\mu_e - 4G_V(\rho_u - \rho_d) + m_{\pi^-}^*. \quad (68)$$

Similarly, the equation for the neutral kaons is given by

$$24 \operatorname{Re} \int \frac{d^3 p}{(2\pi)^3} T \sum_{n=-\infty}^{+\infty} \frac{M_d M_s + \mathbf{p}^2 - (i\omega_n + \mu_d)(i\omega_n + i\Omega_m + \mu_s)}{[(i\omega_n + \mu_d)^2 - \mathbf{p}^2 - M_d^2][(i\omega_n + i\Omega_m + \mu_s)^2 - \mathbf{p}^2 - M_s^2]} = \frac{1}{2K_6^{(+)}}, \quad (69)$$

with

$$Q = \omega + \mu_s - \mu_d = \omega + 4G_V(\rho_d - \rho_s). \quad (70)$$

The in-medium energies are given by

$$\omega_{K^0} = 4G_V(\rho_d - \rho_s) + m_{K^0}^*, \quad (71)$$

$$\omega_{\bar{K}^0} = -4G_V(\rho_d - \rho_s) + m_{\bar{K}^0}^*. \quad (72)$$

We solve Eqs. (60), (65), and (69) by using the values of σ_f and μ_e that correspond to the neutral global minimum

of the effective potential (42). In Fig. 4 we plot the solutions of the real part of the pole equations for charged kaons (upper panels), corresponding to Eqs. (63) and (64); neutral kaons (middle panels), corresponding to Eqs. (67) and (68); and charged pions (lower panels), corresponding to Eqs. (71) and (72). They are plotted against μ for $r_V = 0$ (left-hand panels) and $r_V = +1.1$ (right-hand panels). Results for intermediate values of r_V do not differ qualitatively from those shown in the figure. Also, for negative values of r_V the difference with the case $r_V = 0$ is that the location of the discontinuity in the in-medium energies is shifted to lower values of the quark chemical potential.

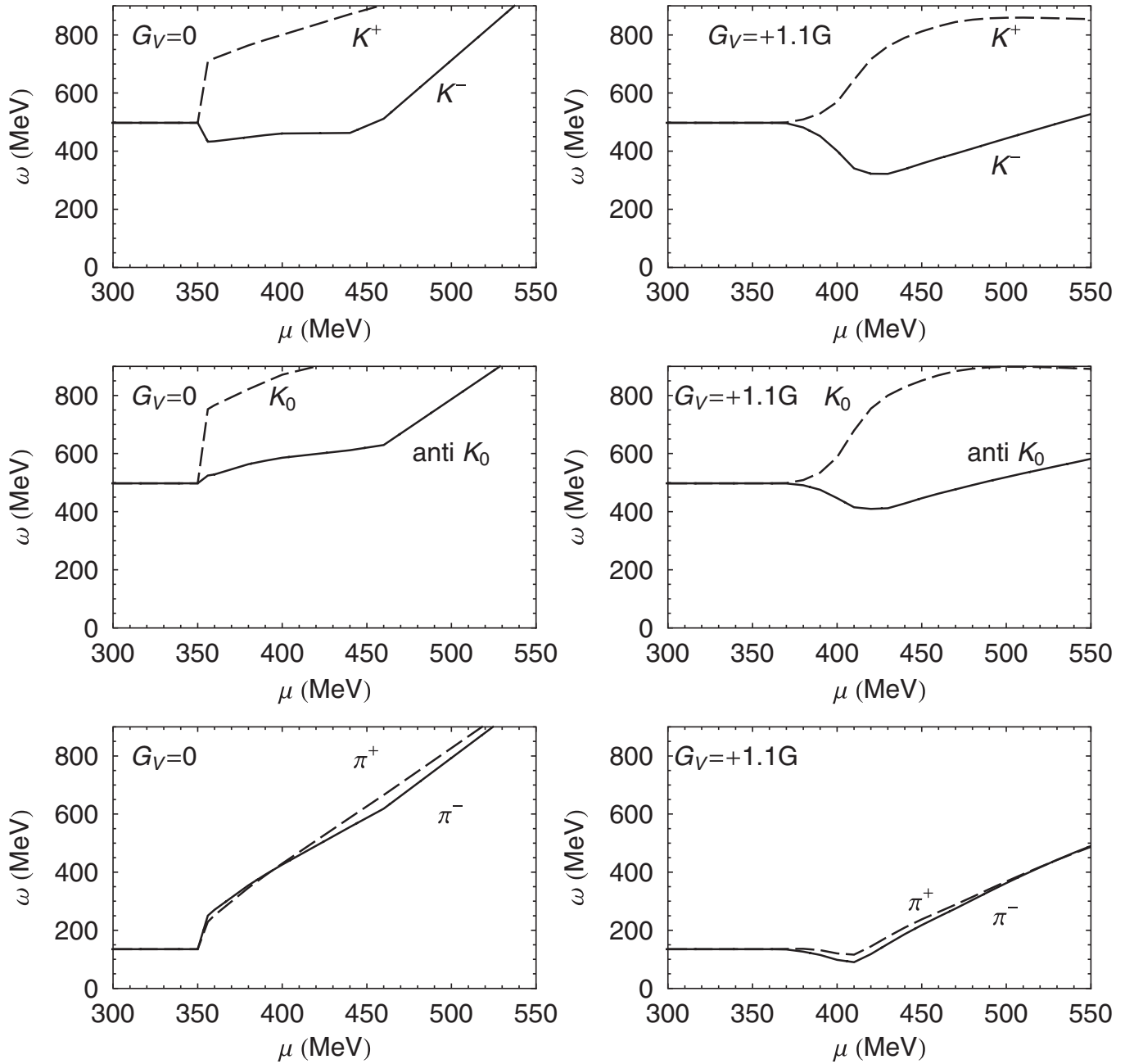


FIG. 4. Solutions of the pole equations in neutral quark matter for charged kaons (upper panel), neutral kaons (middle panel), and charged pions (lower panel) as a function of μ for two different values of r_V .

The plots of Fig. 4 are interesting for several reasons. A general feature of the vector interaction is the stabilization of the charged pseudoscalar states: the comparison at the same chemical potential of the in-medium energies of a meson with and without taking into account the repulsive vector interaction shows that they are higher in the latter case than in the former one. Secondly, we notice that the effect of the vector interaction on the K^- and \bar{K}^0 in-medium energies is to lower them in the μ regime where chiral symmetry is approximately restored. For example, at $\mu = 460$ MeV we find $\omega_{K^-} \approx$

406 MeV for $r_V = 0$, to be compared with $\omega_{K^-} \approx 290$ MeV for $r_V = 1$. This is in part due to a mild lowering of m_K^* as G_V is increased, but mainly to the effective chemical potential arising from interaction of K^- and \bar{K}^0 with the expectation values of the vector meson fields via the quasiquarks in the loop, as is clear in the expressions, Eq. (64) and (72). In the case of K^- there is still a further lowering of the energy due to the larger value of μ_e ; see Fig. 3: at $\mu = 460$ MeV we find $\mu_e \approx 95$ MeV for $r_V = 0$, to be compared with $\mu_e \approx 120$ MeV for $r_V = +1.1$.

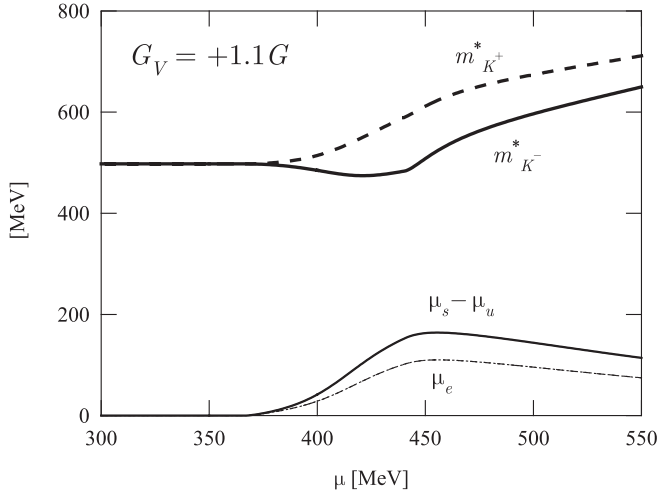


FIG. 5. The various contributions to in-medium kaon energies. Effective in-medium kaon masses $m_{K^\pm}^*$, the electric chemical potential μ_e and $\mu_s - \mu_u$ as a function of μ . $m_{K^\pm}^* \pm (\mu_s - \mu_u)$ correspond to the two curves in the top right-hand figure of Fig. 4. The deviation of $\mu_s - \mu_u$ from μ_e comes from the repulsive vector interaction.

For completeness, in Fig. 5 we plot the separate contributions to the in-medium kaon energies. The solid lines indicated by $m_{K^\pm}^*$ express the in-medium kaon masses while μ_e is the electron chemical potential. The in-

medium kaon mass $m_{K^\pm}^*$ should be compared with $\mu_s - \mu_u = \mu_e + 4G_V(\rho_u - \rho_s)$, which is effective chemical potential felt by K^- : it is shifted from the bare charge chemical potential μ_e means of the vector interaction. Both the electron chemical potential and the vector interaction tend to lower the in-medium K^- energy, even though the lowering is not enough for the kaon condensate to form.

The shape of the inverse K^- propagator at rest as a function of energy and μ has an interesting feature. In Fig. 6 we plot the real and the imaginary part of $F_{K^\pm}(\omega) \equiv 1 - 2K_4^+ \Pi_{K^\pm}(\omega, \mathbf{q} = 0)$ for $r_V = +1.1$ and two values of μ . They are represented, respectively, by the solid line and the dashed line. At $\mu = 0$ we have $\text{Re}F_{K^\pm}(m_K) = \text{Re}F_{K^\pm}(-m_K) = 0$ and $\text{Im}F_{K^\pm}(\omega) = 0$ for $|\omega| < M_u + M_s$. Here m_K denotes the vacuum kaon mass. As μ is increased above the chiral transition, $F_{K^\pm}(\omega)$ develops two singularities at intermediate values of ω ; see the right-hand panel of Fig. 6. Moreover, two new zeros appear. Thus in principle at large μ four kaon modes appear. The solutions we have chosen to draw Fig. 6 are those with the larger magnitude.

In order to make clear the physical content of the intermediate singularities at $\omega = \omega_1, \omega_2$, we will take a detailed look at the imaginary part of $F_{K^\pm}(\omega)$ from now on. It is possible to find some analytic formula for the imaginary part which is physically related to the K^- decay rate in the

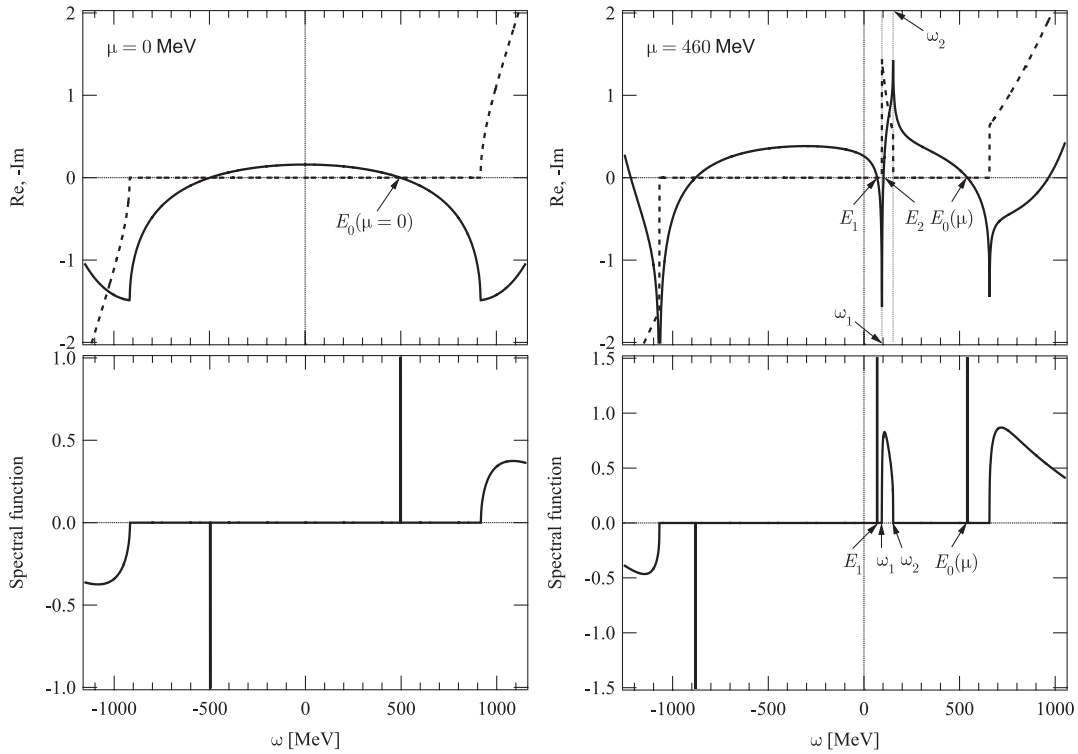


FIG. 6. Upper panel: Real and (minus) imaginary part of $F_{K^\pm}(\omega) \equiv 1 - 2K_4^+ \Pi_{K^\pm}(\omega, \mathbf{q} = 0)$ as a function of ω for $G_V = +1.1G$, for two different values of μ . Solid line corresponds to the real part, dashed line to the imaginary part. Lower panel: Corresponding spectral function of kaonic propagator $\rho(\omega) = \text{Im}(1/F_{K^\pm}(\omega))$.

medium. By use of the formula $\text{Im}(1/(\omega + x + i\delta)) = -i\pi\delta(\omega + x)$, we find

$$\text{Im}F_{K^\pm}(\omega) = -\frac{6K_4^{(+)}}{\pi} \int_0^\infty dp \frac{E_u E_s + M_u M_s + p^2}{E_u E_s} (1 - f_{\bar{u}} - f_s) \delta(Q_0 - E_u - E_s) \quad (73a)$$

$$+ \frac{6K_4^{(+)}}{\pi} \int_0^\infty dp \frac{-E_u E_s + M_u M_s + p^2}{E_u E_s} (f_u - f_s) \delta(Q_0 + E_u - E_s) \quad (73b)$$

$$+ \frac{6K_4^{(+)}}{\pi} \int_0^\infty dp \frac{-E_u E_s + M_u M_s + p^2}{E_u E_s} (f_{\bar{s}} - f_{\bar{u}}) \delta(Q_0 - E_u + E_s) \quad (73c)$$

$$+ \frac{6K_4^{(+)}}{\pi} \int_0^\infty dp \frac{E_u E_s + M_u M_s + p^2}{E_u E_s} (1 - f_u - f_{\bar{s}}) \delta(Q_0 + E_u + E_s), \quad (73d)$$

where Q_0 is again the shifted energy defined by Eq. (61), $E_u = \sqrt{M_u^2 + p^2}$ and $E_s = \sqrt{M_s^2 + p^2}$ are the u and s quark energies, and f 's are the Fermi blocking factors defined by $f_i = \theta(\mu_i - E_i)$ for the quark Fermi distribution, and $f_{\bar{i}} = \theta(-\mu_i - E_i)$ for the antiquark Fermi distribution. Since the momentum integral is definitely convergent, we have removed the cutoff from the evaluation of the imaginary part. As easily guessed from the blocking factors and delta function guaranteeing the energy conservation, (73a) expresses the two body decay from K^- to $(s\bar{u})$, (73b) expresses the Landau damping process of K^- absorbing on-shell u quark decaying into s quark, (73c) represents the inverse Landau damping of K^- absorbing anti- s quark decaying into anti- u quark, and (73d) is for the decay of K^- by absorbing u quark and anti- s quark. The p integral is extremely trivial due to delta functions, yielding

$$\text{Im}F_{K^\pm}(\omega) = -\left[\frac{6K_4^{(+)} p_*}{\pi} \frac{E_u^* E_s^* + M_u M_s + p_*^2}{E_u^* + E_s^*} (1 - f_{\bar{u}} - f_s) \right] \theta[Q_0 > M_u + M_s] \quad (74a)$$

$$+ \left[\frac{6K_4^{(+)} p_*}{\pi} \frac{-E_u^* E_s^* + M_u M_s + p_*^2}{|E_u^* - E_s^*|} (f_u - f_s) \right] \theta[0 < Q_0 < M_s - M_u] \quad (74b)$$

$$+ \left[\frac{6K_4^{(+)} p_*}{\pi} \frac{-E_u^* E_s^* + M_u M_s + p_*^2}{|E_u^* - E_s^*|} (f_{\bar{s}} - f_{\bar{u}}) \right] \theta[-M_s + M_u < Q_0 < 0] \quad (74c)$$

$$+ \left[\frac{6K_4^{(+)} p_*}{\pi} \frac{E_u^* E_s^* + M_u M_s + p_*^2}{E_u^* + E_s^*} (1 - f_u - f_{\bar{s}}) \right] \theta[Q_0 < -M_u - M_s], \quad (74d)$$

where $E_i^{*(*)} \equiv \sqrt{M_i^2 + p_{*(*)}^2}$, and $\{p_*, p_*\}$ are now to be determined through the condition of energy conservation,

$$\begin{aligned} E_u^* + E_s^* &= |Q_0| \quad \text{for } |Q_0| > M_u + M_s, \\ E_s^* - E_u^* &= |Q_0| \quad \text{for } |Q_0| < M_s - M_u, \end{aligned} \quad (75)$$

each of which has a unique solution at fixed Q_0 in its domain of definition. It turns out both have the same functional dependence on Q_0 , i.e.,

$$p_{*(*)} = \frac{\sqrt{((M_s - M_u)^2 - Q_0^2)((M_s + M_u)^2 - Q_0^2)}}{2|Q_0|}. \quad (76)$$

We now consider in which condition the Landau damping process labeled by (74b), $u + K^- \rightarrow s$ [and the inverse production process ($s \rightarrow u + K^-$)] is possible. As demonstrated above, the energy conservation $E_s^* = Q_0 + E_u^*$ has a unique solution when Q_0 is in the interval:

$$0 < Q_0 < M_s - M_u. \quad (77)$$

From Eq. (76), we see p_* is a decreasing function of Q_0 , and when Q_0 approaches zero, p_* diverges. In addition to the energy conservation, the Pauli principle should also be

satisfied: when $p_* > \sqrt{\mu_u^2 - M_u^2}$, or equivalently $E_u^* > \mu_u$, there is no u quark available to contribute to the absorption process $u + K^- \rightarrow s$. This can be also seen in the blocking factor $f_u - f_s$ in Eq. (74b): This factor comes from the sum of two blocking factors, $f_u(1 - f_s)$ for the decay and $-f_s(1 - f_u)$ for the corresponding creation process, $s \rightarrow u + K^-$. Then in order for the total decay rate to be nonzero, either $\{f_u = 1, f_s = 0\}$ or $\{f_u = 0, f_s = 1\}$ should hold. In our case $M_s > M_u$ is always realized so we need to consider only the former condition, that is, $p_{Fs} < p_* < p_{Fu}$, where the Fermi momentum is defined as $p_{Fi} = \sqrt{\max(0, \mu_i^2 - M_i^2)}$. Solving this condition together under the kinematic constraint Eq. (77), we obtain the condition: $\sqrt{M_s^2 + p_{Fu}^2} - \sqrt{M_u^2 + p_{Fu}^2} < Q_0 < \sqrt{M_s^2 + p_{Fs}^2} - \sqrt{M_u^2 + p_{Fs}^2}$, which, combined with $Q_0 = \omega + \mu_s - \mu_u$, translates into

$$\begin{aligned} \omega_1 &= \sqrt{M_s^2 + p_{Fu}^2} - \mu_s - \max(M_u - \mu_u, 0), \\ \omega_2 &= -\sqrt{M_u^2 + p_{Fs}^2} + \mu_u + \max(M_s - \mu_s, 0). \end{aligned} \quad (78)$$

We have checked that these equations reasonably reproduce the numerical values of $\{\omega_1, \omega_2\}$ in the right-hand panel of Fig. 6. We conclude that the imaginary part in the range $\omega_1 < \omega < \omega_2$ is nonvanishing due to the Landau damping of K^- by absorption of on-shell u quark in the system. What is more intriguing is that below this Landau damping threshold, there appears a new pole implying a new collective mode with the same quantum number K^- as shown in Fig. 6. We have checked that this pole appears only at high density, $\mu \lesssim 420$ MeV, as depicted in Fig. 7. At the moment we cannot discern if this new light mode is an artifact of the NJL model itself, as well as of the random phase approximation. However, if this is not the case, it is of great interest since it might change the low temperature behavior of the thermodynamics (e.g., strangeness population) in a compact star. We leave the detailed investigation of the nature of this new pole to a forthcoming paper.

A third point that deserves discussion is the missed symmetry in the K^0/\bar{K}^0 spectrum. This splitting is present even in the case $G_V = 0$. It is due in this case to the fact that $K^0 \sim (d\bar{s})$ and $\bar{K}^0 \sim (s\bar{d})$: on-shell d quarks in the system tend to reduce the binding energy for the K_0 state by Pauli blocking. This is the reason why we see that M_{K_0} is higher than $M_{\bar{K}_0}$. The splitting is more pronounced by the vector interaction, see right-hand panel in Fig. 4, because of the induced effective chemical potential, Eqs. (71) and (72).

We finally comment on the absence of kaon condensation in our model. It is well established that at in the range of baryon densities $(2.3-5)\rho_0$ and for neutral and

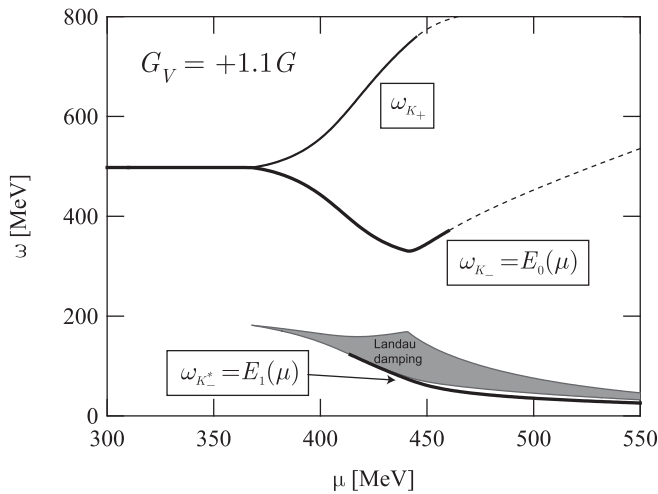


FIG. 7. The energy of the collective modes in the $(\omega-\mu)$ plane. The new collective mode with quantum number K^- induced by the Landau damping. The shaded area corresponds to the region where the response function suffers from imaginary part due to the Landau damping. ω_{K^-} and ω_{K^+} are the same as two curves in the top right-hand figure of Fig. 4. The points where the solid lines turn into the dashed ones indicate the thresholds for the continuum: across the points, the modes become no longer stable, decaying into the constituents.

β -equilibrated nuclear matter, kaon condensation occurs; see, for example, [60–62] and references therein. The main results of [60–62] are in agreement with those that can be obtained within a simple relativistic mean field model [38,39]. In all of these models the numerical value of μ_e at a given baryon density ρ_B is larger (at least a factor of 2) than the μ_e we obtain in our calculations. Also the effective potential felt by kaons and due to interactions with ρ and ω mesons is enhanced in neutral nuclear matter, while in the model we study here it has only a mild dependence on ρ_B . We guess that these two factors are the main source of difference between our results and the nuclear matter literature. At the moment we have not yet found a solution for this problem. A first possibility could be the hadronization of the NJL model [23], that would allow one to describe the system in terms of protons and neutrons instead of quarks. Probably the neutralization and β equilibration of this system would result in a larger value of μ_e . Secondly, the expansion of the effective action of the meson fields to higher orders would introduce in the theory the direct coupling of kaons with ω and ρ mesons. However, a dimensional analysis shows that these contributions are parametrically suppressed by powers of $\langle\omega_0\rangle/m_K$; thus, they should not be important. In order to verify this, a direct calculation of the relevant diagrams should be performed. Thirdly, we cannot exclude that multiquark interactions, that are known to be useful in the stabilization of nuclear matter [22,32,63], can play a role in increasing the strength of the effective kaon potentials. Tensor interactions might also lead to an enhancement of the attractive interaction felt by the kaons in the medium. Last (but not the least), there is the possibility to include a density dependence of G_V via a fit to experimental data on the ω meson mass [33]. Some of these aspects are under current investigation.

VI. VECTOR INTERACTION AND COLOR SUPERCONDUCTIVITY

We briefly comment on the effect that our results might have on color superconductivity [64–67]. At large baryon density color superconductive phases, neglected in this paper for simplicity, could play a relevant role in the determination of the ground state. In the two flavor case the interactions in the quark-antiquark and diquark channels have been considered, for example, in Ref [35]. In order to understand how vector interaction can interplay with superconductivity in the three flavor model under investigation here, we compare the various quark densities at $\mu = 550$ MeV for $r_V = 0$ and $r_V = 1.1$; see Fig. 8.

In the case $r_V = 0$ we find $\rho_u \approx 12.9\rho_0$, $\rho_d \approx 14.2\rho_0$, $\rho_s \approx 11.6\rho_0$; the in-medium quark masses are $M_u \approx M_d \approx 7$ MeV and $M_s \approx 197$ MeV; the Fermi momenta of the different flavors are $p_F^u \approx 538$ MeV, $p_F^d \approx 556$ MeV, and $p_F^s \approx 520$ MeV. It is well established that in these conditions quarks condense to the color-flavor-

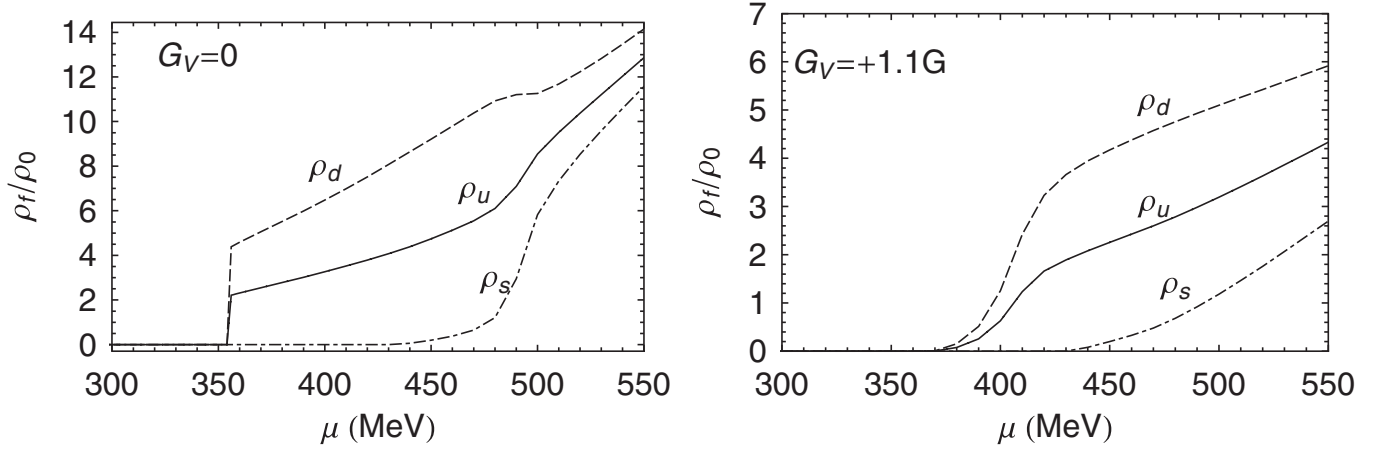


FIG. 8. Quark number densities against μ for $r_V = 0$ (left-hand panel) and $r_V = +1.1$ (right-hand panel).

locked phase state [50,68,69]. On the other hand, for the case $r_V = 1.1$ we find $\rho_u \approx 4.35\rho_0$, $\rho_d \approx 5.95\rho_0$, $\rho_s \approx 2.71\rho_0$; the in-medium quark masses are $M_u \approx M_d \approx 20$ MeV and $M_s \approx 390$ MeV; the Fermi momenta of the different flavors are $p_F^u \approx 374$ MeV, $p_F^d \approx 415$ MeV, and $p_F^s \approx 320$ MeV. It is not clear in this case which superconductive state could be favored, if any, since a self-consistent calculation in color superconductivity that takes into account the vector interaction is missing in the three flavor case.

If we suppose that color superconductivity sets in, in order to guess which state could be a good candidate in these conditions we compute the ratio M_s^2/μ . We find $M_s^2/\mu \approx 276$ MeV. In these conditions, since $p_F^u - p_F^s \approx p_F^d - p_F^u \approx 2(p_F^d - p_F^s) \approx 50$ MeV, probably the three flavor crystalline Larkin-Ovchinnikov-Fulde-Ferrel phase state is the best candidate in the weak coupling regime [51,70–72]. If the diquark coupling is high enough at this value of the chemical potential, then a two flavor color superconductive phase could be the ground state. In addition to this, there is probably room for spin-1 condensates. We also guess that because of the smooth crossover (see right-hand panel of Fig. 8) and the nontrivial coupling between the diquark and meson excitations a coexistence region might be created, as already discussed in Refs. [35,73]. Of course these are just some of the possibilities that should be either supported or not by a dynamical calculation. We notice finally that our reasonings are not beyond the capabilities of the model even if we take $\mu = 550$ MeV since the Fermi momenta in the case $r_V = 1.1$ are quite small compared to the ultraviolet cutoff Λ (they are smaller than the vacuum kaon mass).

VII. CONCLUSIONS

We have explored the consequence of the vector interaction in β -equilibrated and neutral three flavor quark matter at finite density. Neutrality and β equilibrium are

required to reproduce the conditions that could be realized in cold neutron stars. The extension of the NJL model to the VENJL one has not only an academic interest. As a matter of fact, in view of vector manifestation the vector mesons can play a relevant role in the restoration of chiral symmetry at large baryon density [26,27]. Moreover, if we wish to describe the intermediate baryon density region of the NJL phase diagram in terms of a bosonized (and eventually hadronized) action, we need to take into account the effects of ω and ρ meson exchange to be more realistic.

Even if it is possible to choose the value of the vector coupling G_V in the vacuum, it is not clear what its value is in the medium. For this reason we have fixed the scalar coupling G and treated the ratio $r_V = G_V/G$ as a free parameter. We have found the interesting result that there exists a critical value of $r_V \approx 0.5$ above which the approximate chiral restoration becomes a crossover (at $r_V = 0$ the NJL model predicts a first order transition). This result is summarized in Fig. 1. Our result is in agreement with Klimt, Lutz, and Weise [19] and with Fukushima [31], where neutrality and β equilibrium were not required.

We have also started a systematic study of the meson energies as a function of the baryon density and on the influence of the vector coupling, focusing in this explorative work on the pseudoscalar channels and leaving a more complete study to a future project. In particular, our findings on the K^- energy show that kaon condensation is quite hard to realize within the present version of the model. This is in disagreement with other results [38,39,60–62], but we argue that the source of the disagreement is mainly the still poor description of the meson-quark interactions in matter at densities of the order of few times ρ_0 that we have within the VENJL model. We have itemized some improvements that might lead to a better description of matter in the intermediate density region, and some of the aforementioned research lines are currently under investigation.

ACKNOWLEDGMENTS

We acknowledge P. Colangelo for a careful reading of the manuscript and for interesting discussions, and M. V. Carlucci for her kind assistance in the preparation of some

of the figures. We also acknowledge discussions with C. Manuel on the topics discussed in this paper. The work of H.A. was supported by the Alexander von Humboldt Foundation.

-
- [1] C. R. Allton *et al.*, Phys. Rev. D **66**, 074507 (2002).
 [2] R. V. Gavai and S. Gupta, Phys. Rev. D **68**, 034506 (2003).
 [3] Z. Fodor and S. D. Katz, J. High Energy Phys. **04** (2004) 050.
 [4] P. de Forcrand and O. Philipsen, Nucl. Phys. **B642**, 290 (2002).
 [5] M. D'Elia and M. P. Lombardo, Phys. Rev. D **70**, 074509 (2004).
 [6] Y. Nambu and G. Jona-Lasinio, Phys. Rev. **122**, 345 (1961); **124**, 246 (1961).
 [7] S. P. Klevansky, Rev. Mod. Phys. **64**, 649 (1992).
 [8] T. Hatsuda and T. Kunihiro, Phys. Rep. **247**, 221 (1994).
 [9] M. Buballa, Phys. Rep. **407**, 205 (2005).
 [10] K. Fukushima, Phys. Lett. B **591**, 277 (2004).
 [11] C. Ratti, M. A. Thaler, and W. Weise, Phys. Rev. D **73**, 014019 (2006).
 [12] C. Ratti, S. Roessner, and W. Weise, Phys. Lett. B **649**, 57 (2007).
 [13] Y. Sakai, K. Kashiwa, H. Kouno, and M. Yahiro, Phys. Rev. D **77**, 051901 (2008); **78**, 036001 (2008).
 [14] G. 't Hooft, Phys. Rev. Lett. **37**, 8 (1976); Phys. Rev. D **14**, 3432 (1976); **18**, 2199 (1978).
 [15] M. Kobayashi and T. Maskawa, Prog. Theor. Phys. **44**, 1422 (1970); M. Kobayashi, H. Kondo, and T. Maskawa, Prog. Theor. Phys. **45**, 1955 (1971).
 [16] V. Bernard and U. G. Meissner, Nucl. Phys. **A489**, 647 (1988).
 [17] M. Asakawa and K. Yazaki, Nucl. Phys. **A504**, 668 (1989).
 [18] S. Klimt, M. Lutz, U. Vogl, and W. Weise, Nucl. Phys. **A516**, 429 (1990).
 [19] S. Klimt, M. Lutz, and W. Weise, Phys. Lett. B **249**, 386 (1990).
 [20] R. Nasseripour *et al.* (CLAS Collaboration), Phys. Rev. Lett. **99**, 262302 (2007).
 [21] M. Naruki *et al.*, Phys. Rev. Lett. **96**, 092301 (2006).
 [22] W. Bentz and A. W. Thomas, Nucl. Phys. **A696**, 138 (2001).
 [23] W. Bentz, T. Horikawa, N. Ishii, and A. W. Thomas, Nucl. Phys. **A720**, 95 (2003).
 [24] M. Harada and K. Yamawaki, Phys. Lett. B **297**, 151 (1992).
 [25] M. Harada and K. Yamawaki, Phys. Rev. D **64**, 014023 (2001).
 [26] M. Harada and K. Yamawaki, Phys. Rep. **381**, 1 (2003).
 [27] M. Harada and K. Yamawaki, Phys. Rev. Lett. **86**, 757 (2001).
 [28] N. Yamamoto, M. Tachibana, T. Hatsuda, and G. Baym, Phys. Rev. D **76**, 074001 (2007).
 [29] M. Lutz, S. Klimt, and W. Weise, Nucl. Phys. **A542**, 521 (1992).
 [30] M. Kitazawa, T. Koide, T. Kunihiro, and Y. Nemoto, Prog. Theor. Phys. **108**, 929 (2002).
 [31] K. Fukushima, Phys. Rev. D **77**, 114028 (2008); **78**, 039902 (2008).
 [32] R. Huguet, J. C. Caillon, and J. Labarsouque, Nucl. Phys. **A781**, 448 (2007).
 [33] R. Huguet, J. C. Caillon, and J. Labarsouque, Phys. Rev. C **75**, 048201 (2007).
 [34] K. Kashiwa, H. Kouno, T. Sakaguchi, M. Matsuzaki, and M. Yahiro, Phys. Lett. B **647**, 446 (2007).
 [35] K. Kashiwa, M. Matsuzaki, H. Kouno, and M. Yahiro, Phys. Lett. B **657**, 143 (2007).
 [36] M. Lutz, A. Steiner, and W. Weise, Phys. Lett. B **278**, 29 (1992).
 [37] D. B. Kaplan and A. E. Nelson, Phys. Lett. B **175**, 57 (1986); for a review, see, for example, T. Muto, Prog. Theor. Phys. Suppl. **153**, 174 (2004).
 [38] N. K. Glendenning, *Nuclear Physics, Particle Physics and General Relativity* (Springer, New York, 1997), p. 390.
 [39] M. Prakash, I. Bombaci, M. Prakash, P. J. Ellis, J. M. Lattimer, and R. Knorren, Phys. Rep. **280**, 1 (1997).
 [40] T. Roth, M. Buballa, and J. Wambach, arXiv:nucl-th/0504056.
 [41] S. B. Ruster, V. Werth, M. Buballa, I. A. Shovkovy, and D. H. Rischke, Phys. Rev. D **73**, 034025 (2006).
 [42] F. Sandin and D. Blaschke, Phys. Rev. D **75**, 125013 (2007).
 [43] H. Abuki, T. Brauner, and H. J. Warringa, arXiv:0901.2477.
 [44] V. Laporta and M. Ruggieri, Phys. Lett. B **633**, 734 (2006); **637**, 374 (2006).
 [45] A. A. Belkov, A. V. Lanyov, and A. Schaale, arXiv:hep-ph/9307331.
 [46] E. Ruiz Arriola and L. L. Salcedo, Nucl. Phys. **A590**, 703 (1995).
 [47] V. Bernard, A. H. Blin, B. Hiller, Y. P. Ivanov, A. A. Osipov, and U. G. Meissner, Ann. Phys. (N.Y.) **249**, 499 (1996).
 [48] L. y. He, M. Jin, and P. f. Zhuang, Phys. Rev. D **71**, 116001 (2005).
 [49] H. Abuki, R. Anglani, R. Gatto, M. Pellicoro, and M. Ruggieri, Phys. Rev. D **79**, 034032 (2009).
 [50] S. B. Ruster, V. Werth, M. Buballa, I. A. Shovkovy, and D. H. Rischke, Phys. Rev. D **72**, 034004 (2005).
 [51] N. D. Ippolito, G. Nardulli, and M. Ruggieri, J. High Energy Phys. **04** (2007) 036.
 [52] J. B. Kogut and D. Toublan, Phys. Rev. D **64**, 034007 (2001).

- [53] A. Barducci, R. Casalbuoni, G. Pettini, and L. Ravagli, *Phys. Rev. D* **71**, 016011 (2005).
- [54] H. J. Warringa, D. Boer, and J. O. Andersen, *Phys. Rev. D* **72**, 014015 (2005).
- [55] A. Ramos, J. Schaffner-Bielich, and J. Wambach, *Lect. Notes Phys.* **578**, 175 (2001).
- [56] D. Ebert, K. G. Klimenko, V. C. Zhukovsky, and A. M. Fedotov, *Eur. Phys. J. C* **49**, 709 (2007).
- [57] D. Ebert and K. G. Klimenko, *Eur. Phys. J. C* **46**, 771 (2006).
- [58] D. Ebert and K. G. Klimenko, *J. Phys. G* **32**, 599 (2006).
- [59] T. Muto and T. Tatsumi, *Phys. Lett. B* **283**, 165 (1992).
- [60] V. Thorsson, M. Prakash, and J. M. Lattimer, *Nucl. Phys.* **A572**, 693 (1994); **A574**, 851 (1994).
- [61] G. E. Brown, C. H. Lee, H. J. Park, and M. Rho, *Phys. Rev. Lett.* **96**, 062303 (2006).
- [62] G. E. Brown, C. H. Lee, and M. Rho, *Phys. Rep.* **462**, 1 (2008).
- [63] I. N. Mishustin, L. M. Satarov, and W. Greiner, *Phys. Rep.* **391**, 363 (2004).
- [64] D. Bailin and A. Love, *Phys. Rep.* **107**, 325 (1984).
- [65] M. G. Alford, K. Rajagopal, and F. Wilczek, *Phys. Lett. B* **422**, 247 (1998).
- [66] R. Rapp, T. Schafer, E. V. Shuryak, and M. Velkovsky, *Phys. Rev. Lett.* **81**, 53 (1998).
- [67] M. G. Alford, K. Rajagopal, and F. Wilczek, *Nucl. Phys.* **B537**, 443 (1999).
- [68] H. Abuki, M. Kitazawa, and T. Kunihiro, *Phys. Lett. B* **615**, 102 (2005); H. Abuki and T. Kunihiro, *Nucl. Phys.* **A768**, 118 (2006).
- [69] D. Blaschke, S. Fredriksson, H. Grigorian, A. M. Oztas, and F. Sandin, *Phys. Rev. D* **72**, 065020 (2005).
- [70] R. Casalbuoni, R. Gatto, N. Ippolito, G. Nardulli, and M. Ruggieri, *Phys. Lett. B* **627**, 89 (2005); **634**, 565 (2006).
- [71] M. Mannarelli, K. Rajagopal, and R. Sharma, *Phys. Rev. D* **73**, 114012 (2006).
- [72] K. Rajagopal and R. Sharma, *Phys. Rev. D* **74**, 094019 (2006).
- [73] D. Zablocki, D. Blaschke, and R. Anglani, *AIP Conf. Proc.* **1038**, 159 (2008).